A Tunable, Stable, and Bioactive MOF Catalyst for Generating a Localized Therapeutic from Endogenous Sources

*Jacqueline L. Harding, Jarid M. Metz, and Melissa M. Reynolds**

The versatile chemical and physical properties of metal organic frameworks (MOFs) have made them unique platforms for the design of biomimetic catalysts, but with only limited success to date due to instability of the MOFs employed in physiological environments. Herein, the use of Cu(II)1,3,5-Benzene-tris-triazole (CuBTTri) is demonstrated for the catalytic generation of the bioactive agent nitric oxide (NO) from endogenous sources, *S*-nitrosothiols (RSNOs). CuBTTri exhibits structural integrity in aqueous environments, including phosphate buffered saline (76 h, pH 7.4, 37 °C), cell media used for in vitro testing (76 h, pH 7.4, 37 °C), and fresh citrated whole blood (30 min, pH 7.4, 37 °C). The application of CuBTTri for use in polymeric medical devices is explored through the formation of a composite CuBTTri-poly by blending CuBTTri into biomedical grade polyurethane matrices. Once prepared, the CuBTTri-poly material retains the catalytic function towards the generation of NO with tunable release kinetics proportional to the total content of CuBTTri embedded into the polymeric material with a surface flux corresponding to the therapeutic range of 1–100 nM cm^{-2} min^{-1}, which is maintained even following exposure to blood.

1. Introduction

Medical devices are invaluable for the restoration of natural function to body parts that have been damaged as a result of disease or injury. However, current technology used in the fabrication of devices is subject to a high risk of infection and also negative interfacial responses, collectively termed biofouling.[1] Device biofouling accounts for 65% of chronic nosocomial infections that are often resistant to antibiotic treatment.[2] In addition, following implantation, continuous administration of antifouling medications is necessary for the lifetime of the device in an attempt to minimize fouling associated with device failure.[3] Reasons for implanted device failure are recurrently attributed to the material's inability to maintain an environment that mimics the function of the surrounding vasculature.[4] As such, it is critical to design devices create an environment which mediates device biofouling while promoting the regeneration of healthy tissues.

J. L. Harding, J. M. Metz, Prof. M. M. Reynolds
Colorado State University
Department of Chemistry
1872 Campus Delivery
Fort Collins, CO 80523
E-mail: Melissa.Reynolds@colostate.edu

DOI: 10.1002/adfm.201402529

Inspired design of new biomaterials uses bioactive agents to mediate the surface properties of implanted devices.[5] Nitric oxide (NO) is perhaps the most ubiquitous of all bioagents responsible for maintaining cellular homeostasis[6] and mounting immune responses.[7] Current NO-release biomaterials exhibit antimicrobial properties,[8] inhibit the deposition of platelets,[9] and promote the regeneration of healthy tissues.[10] However, current NO-release materials remain limited by the lifetime of the incorporated NO reservoir, which is a significant drawback for applications that require long-term implantation and function.[11]

As an alternative, biocatalysts for the generation of NO that rely on a physiologically derived source promise to be effective for long-term applications in which they regulate antifouling effects and promote cellular regeneration. Continuous generation of NO across all healthy tissues occurs naturally via NO synthase and L-arginine.[12] However, there is debate over the exact mechanism of action. Rather than develop a material that mimics the enzymatic generation of NO, we hypothesized that one can capitalize on *S*-nitrosothiols (RSNOs) that are storage and transport vehicles for NO in the blood stream (10–100 μM).[13] Bioavailable small molecule RSNOs are formed at the thiol moieties of cysteine derivatives, where reaction with solvated- or protein-bound sources of Cu^{2+} ions catalyze the release of NO described by Equation 1.[14,15] As such, polymeric materials with embedded Cu^{2+} catalyst sites either as small molecule catalysts and macromolecular zeolites have been explored to facilitate the surface-localized generation of NO in order to modulate the onset of device biofouling.[16]

$$2\mathrm{RSNO} \xrightarrow{Cu^{2+}} 2\mathrm{NO} + \mathrm{RSSR} \quad (1)$$

Metal organic frameworks (MOFs) are robust crystalline materials with amendable chemical and physical properties that result in versatility for a wide range of applications, including small molecule sequestering/storage,[16] membrane separations,[17] and heterogeneous catalysts,[18] to name a few. As a result, MOFs have generated significant interest as platforms for biomedical applications, but with only limited success to date due to instability of the MOFs employed in physiological environments.[19] Fortunately, the versatility of MOFs provides

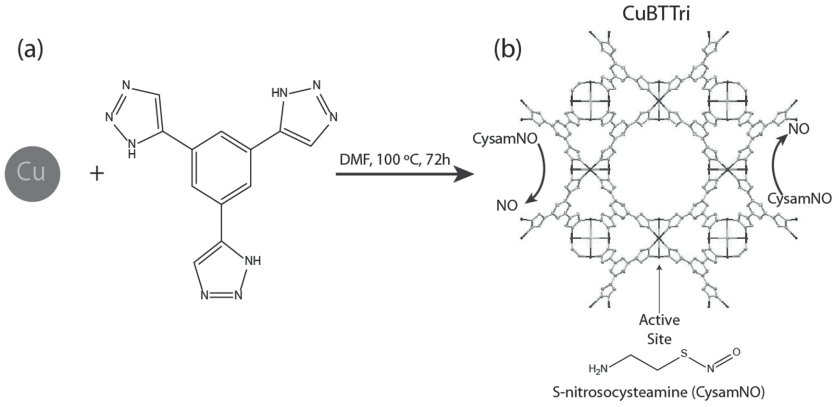

Figure 1. MOF biocatalyst, CuBTTri, for the catalytic generation of nitric oxide from bioavailable substrates. a) Synthesis of CuBTTri, b) Reactivity of CuBTTri with S-nitrosocysteamine (CysamNO).

nearly limitless combinations of metal ions and ligands which allows a route to tunable physical and chemical properties.[20] The use of azole based ligands is reported to have improved stability in aqueous environments compared to their carboxylate counterparts, even under strongly acidic and basic conditions.[21] In previous work, we demonstrate the successful implementation of the archetypal MOF CuBTC as a catalyst for the generation of NO from endogenous RSNO substrates, although stability in an aqueous system was elusive.[22] Towards the goal of implementing MOFs in a biological environment for the catalytic generation of NO, we selected the previously reported water-stable MOF, CuBTTri, which contains coordinatively unsaturated Cu^{2+} metal centers linked by 1,3,5-benzene tris triazole moieties, as shown in **Figure 1**b.[23] While there are numerous reports of CuBTTri as an excellent material for the adsorption of CO_2[23,24] our aim in the present studies was to broaden the scope of CuBTTri applicability for use as a biocatalyst.

Herein, we demonstrate the catalytic potential of CuBTTri as a NO catalyst with the RSNO substrate, *S*-nitrosocysteamine (CysamNO) according to Equation 2 and shown schematically in Figure 1. Subsequently, we determined via pXRD that the crystalline integrity of CuBTTri was maintained following reaction with CysamNO and in mediums routinely used for in vitro and in vivo experiments, including phosphate buffered saline (PBS), cell media, and whole blood. The development of a composite material with CuBTTri blended into biomedical polyurethane resulted in the capacity for localized catalytic generation of NO as a therapeutic. Furthermore, kinetic control over the NO dosage is feasible and here we demonstrate the capacity for tuning the NO surface flux of the material to lie within the physiologically relevant range.

$$2\mathrm{RSNO} \xrightarrow{\mathrm{CuBTTri}} 2\mathrm{NO} + \mathrm{RSSR} \quad (2)$$

2. Catalytic Activity of CuBTTri

The catalytic activity of CuBTTri towards the generation of NO when reacted with CysamNO in PBS was monitored in situ using chemiluminescence detection. The reactivity of CuBTTri was evaluated by comparing the rate of NO generation in the absence of a catalyst and with solvated Cu^{2+} ions as controls (**Figure 2**). The average rate of NO generation in PBS at 25 °C when catalyzed by CuBTTri is 22.8 ± 2.1 nM s^{-1} and is an order of magnitude greater than the uncatalyzed reaction at 2.9 ± 0.6 nM s^{-1} (**Table 1**). Comparatively, in the presence of solvated Cu^{2+} ions (Equation 1) the rate of the reaction increases an additional order of magnitude to 333.0 ± 5.1 nM s^{-1} when compared to CuBTTri. These results are consistent with the previous reports of the reactivity of solvated Cu^{2+} catalysts with RSNOs.[15] Specifically, Cu-MOF catalysts with RSNOs have shown the same reactivity trend.[22]

We further investigated the influence of the catalyst content with regard to substrate concentration on the rate of NO release (**Figure 3**). First, the influence of substrate concentration on the rate of NO generation was explored when the reaction content of the catalyst remained consistent as shown in Figure 3a. In these experiments, the rate of the reaction increased linearly as the concentration of the substrate was increased; however, the reaction with respect to CysamNO proceeded via zero-order reaction kinetics, shown in (Figure S1, Supporting Information). Interestingly, in each case the amount of NO recovered was equal to 50% of the substrate conversion, leading to total turnover numbers ranging between 1.06 ± 0.04 to 3.90 ± 0.16, shown in Table 1. Notably, even when the reaction content of CuBTTri was in excess of the substrate, the conversion to NO remained consistent at 50% and is attributed to the reaction reaching an equilibrium state with the substrate and the resulting disulfide product. This hypothesis was confirmed by the subsequent addition of a 2 equivalent aliquot of CysamNO to the spent reaction solution where NO release proceeded with only 25% of the second aliquot reacting in solution. As shown in Figure 3b, as the catalyst content in the reaction was

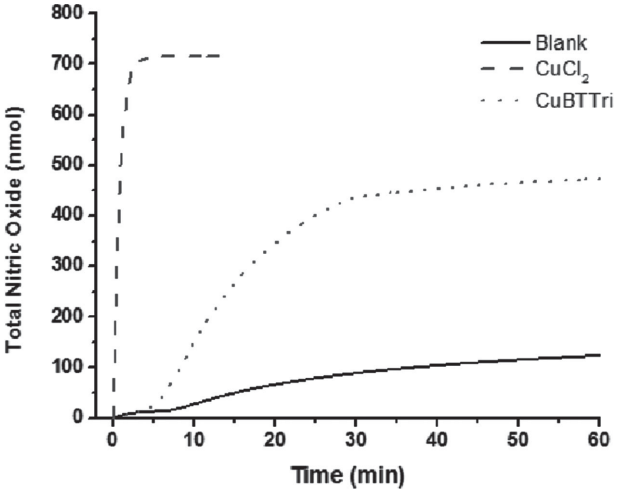

Figure 2. Comparison of Total NO release rates between CuBTTri, uncatalyzed CysamNO decomposition, and solvated Cu^{2+} ions.

Table 1. Summary of rate of NO generation[a)]

Catalyst[b)]	CysamNO [mM]	CysamNO:Cu^{2+}	NO Release Rate (nM s^{-1})	Total Turnovers
None	0.50	n/a	2.88 ± 0.58	n/a
CuBTTri	0.25	2:1	17.3 ± 2.54	1.06 ± 0.04
CuBTTri	0.50	4:1	22.8 ± 2.08	1.90 ± 0.16
CuBTTri	1.0	8:1	24.2 ± 2.32	3.90 ± 0.16
CuCl2	0.50	4:1	333 ± 5.10	1.43 ± 0.03

[a)]All experiments performed in PBS (2 mL, pH 7.4, 25 °C) at $n = 3$ and reported at 95% confidence interval;[b)] Catalyst content CuBTTri (0.2 mg, 5×10^{-7} mol Cu^{2+}) and $CuCl_2$ (5×10^{-7} mol Cu^{2+})

increased, there was a linear correlation with the rate of NO release with second-order kinetics being followed, data shown in Supporting Information (Figure S2, Supporting Information). Taken together, these results indicate that CuBTTri successfully executes the role of a catalyst towards NO generation with RSNOs that is not impeded by mass-transfer effects or diffusion limitations.

Critical challenges in the development of NO releasing therapeutic materials are often due the difficultly in tuning NO delivery kinetics for therapeutic effectiveness. Additionally, it is critical to overcome the finite amounts of NO that can be incorporated into the material, which currently limit the active lifetime of the material.[11] Advantageously the use of a catalyst for NO generation which relies on the endogenous reservoirs of NO in the blood stream have the potential for exhibiting NO release for the lifetime of implanted materials. Furthermore the use of CuBTTri as a catalyst imparts the capacity for kinetic control over the amount of NO generated facilitating tunable dosages of NO for therapeutic applications regardless of the likely fluctuation of RSNOs in the blood stream.

3. Heterogeneous vs Homogenous Catalyzed Reaction: Assessment of MOF Structural Stability

The resistance of CuBTTri towards degradation under aqueous conditions is critical towards the sustained use of the material as a catalyst. Towards this end, we assessed the structural integrity of the catalyst based on the retained crystallinity of the material by powder X-ray diffraction and by elemental analysis of the post-reaction filtrate for residual Cu^{2+} ions (Table S1, Supporting Information). Evaluation of the soaking solution for Cu^{2+} content following

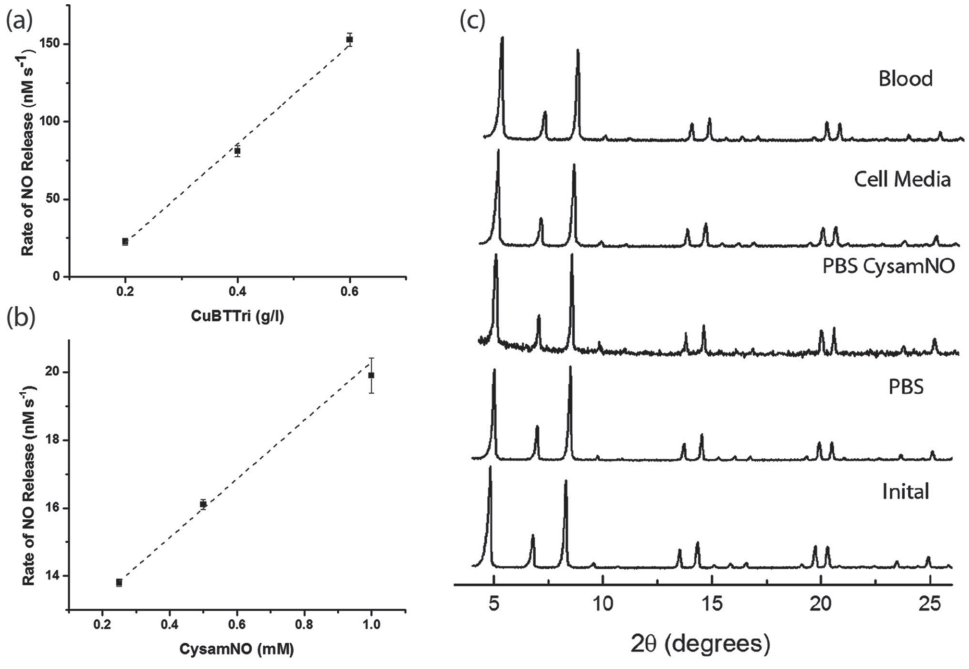

Figure 3. Reactivity and stability of CuBTTri catalyst. a) Rate of NO generation from CysamNO (0.5 mM) in PBS (2 mL) catalyzed by CuBTTri at 25 °C. b) Rate of NO generation from CysamNO catalyzed by CuBTTri (0.2 mg) in PBS (2 mL) at 25 °C. Values ($n = 3$) and standard deviations reported to the 95% confidence interval. c) Powder X-ray diffraction patterns of parent CuBTTri particles compared with CuBTTri particles immersed in PBS (37 °C, pH 7.4); 5 mM CysamNO in PBS (37 °C, pH 7.4); Endothelial cell media (37 °C, pH 7.4 maintained with 5% CO_2 buffer); Fresh citrated whole blood (37 °C, pH 7.4).

the reaction indicated that 0.04 ± 0.01% of the available Cu^{2+} ions from the initial CuBTTri added to the reaction is accounted for in the filtered reaction solution. At this concentration of Cu^{2+} ions, the rate of NO release from CysamNO is the same as that of the uncatalyzed reaction within experimental error, indicating that the observed increase in the rate of NO release is associated with Cu^{2+} ions bound in the CuBTTri framework. Assessment of MOFs using pXRD is an established method for indicating the structural integrity of the material based on the capacity of the material to retain its original crystallinity. In comparison to the parent diffraction pattern, when CuBTTri particles were immersed in PBS at 37 °C for 72 h, the CuBTTri particles post reaction with CysamNO (0.5 mM in PBS) retained their original diffraction pattern, as shown in Figure 3c. Since, the assembly of MOFs require the use of specific reaction conditions to achieve a particular topology, the dissolution of the framework and subsequent recrystallization is not likely to result. Hence, the implied conclusion is that the framework is retaining heterogeneous character over the course of the reaction. In short, tunable release kinetics of a therapeutic agent from an endogenous source plus unprecedented stability of a MOF in PBS solution makes CuBTTri an excellent candidate for exploration in biotherapeutic applications.

3.1. Stability of CuBTTri Under In Vitro and In Vivo Conditions

The integration of MOFs in a biological setting further requires the evaluation of CuBTTri stability in cell media solutions used for in vitro testing and, most importantly, in body fluids. Hence, the crystallinity of CuBTTri was assessed after immersion in endothelial cell media maintained at pH 7.4 by a 5% CO_2 atmosphere for 72 h and in a separate experiment, following brief exposure (30 min) to fresh citrated whole blood the crystallinity was assessed. The representative diffraction patterns (Figure 3c) indicate that the structural integrity of the material was preserved. This is an important result because minimal biodegradation of CuBTTri has the potential to extend the lifetime of material use while minimizing toxicity associated risks. While rigorous in vitro and in vivo testing remains to be done to determine any toxicity associated with CuBTTri, Cu remains an essential trace element in physiology rendering the body capable of uptake and clearance of MOF degradation products.[25]

4. Composite CuBTTri Biomedical Grade Polyurethanes

The administration of MOFs in biomedicine is achieved either through bulk administration in the blood stream or through the formation of composite materials. Composite materials are particularly advantageous in that they have the flexibility to be incorporated into a wide range of existing polymeric medical devices. Moreover, the immobilization in device matrices is expected to facilitate the site-localized delivery of the therapeutic. The high reactivity of NO necessitates site specific generation at the intended physiological site. Hence, we explored the activity of CuBTTri towards catalytic NO generation once embedded into a matrix of biomedical grade polyurethane. CuBTTri-poly films were prepared by incorporating CuBTTri at 1 or 4 wt% into a solution of THF solvated polyurethane polymer, followed by subsequent casting into 4 mm circular molds. Additionally, the robustness of CuBTTri following exposure to organic solvents used in the preparation of polymeric materials was demonstrated after exposing CuBTTri to THF for 24 h at room temperature by ex situ pXRD (Figure S3, Supporting Information). Examination of CuBTTri-polymer by SEM is shown in **Figure 4**, indicating that there are MOF particles on the surface the material, but that the majority of

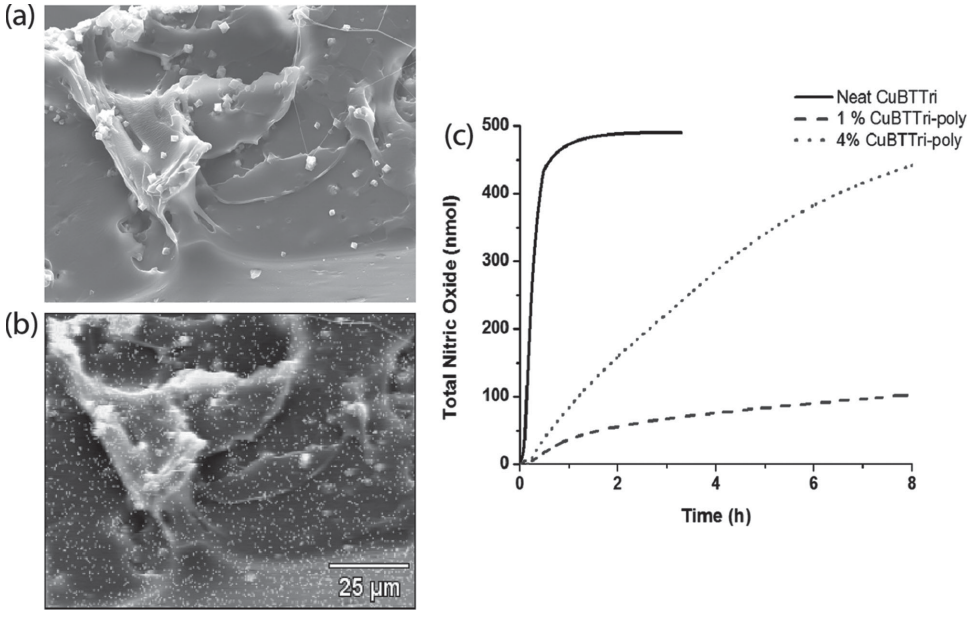

Figure 4. a) SEM of CuBTTri- poly films at 1000× magnification, b) SEM-EDX mapping of Cu content in CuBTTr-poly films at 1000× magnification, and c) total NO release from CysamNO, CuBTTri, 4% CuBTTri-poly film, 1% CuBTTri-poly film. Values ($n = 3$) and standard deviations reported to the 95% confidence interval.

MOF particles remain embedded within the polymeric matrix. Dispersion of the CuBTTri particles throughout the polymeric matrix was assessed by analyzing the material for Cu content using SEM analysis accompanying energy dispersive X-ray analysis. As shown in Figure 4b, there is a relatively even dispersion of Cu atoms throughout the material, indicating that the CuBTTri particles are embedded within the polymer matrix.

4.1. Catalytic Activity of CuBTTri-Poly Materials

The catalytic generation of CuBTTri once embedded into the polymeric matrix was evaluated by reacting 1 and 4 wt% CuBTTri-polymeric materials with CysamNO in PBS. To deduce the effects of encapsulation on the reactivity of CuBTTri, we compared the rate of NO generation between the free CuBTTri particles and the 4% CuBTTri films using an equivalent amount of CuBTTri (0.5 μmol Cu^{2+}) in each experiment. The results show that the rate of NO release is reduced 8-fold once the material is incorporated into the polymeric matrix in the otherwise identical reaction to that observed with the non-embedded particles. The slowed reactivity of the polymer-encapsulated cuber is the expected result of diffusion limitations of the substrate towards reaching the CuBTTri active sites. Reducing the total amount of CuBTTri incorporated into the polymeric matrix further reduces the rate of NO generation from CysamNO, which is consistent with our findings that kinetic control over the amount of NO generated is based on the availability of the catalyst, shown in Figure 4c. Following the reaction of the composite material with CysamNO, the reaction solution was evaluated by ICP-MS for Cu content in order to establish the extent of CuBTTri leaching from the polymer membrane. For both the 1% and 4% films, ≤0.47 ± 0.03% of the available Cu^{2+} ions were found in solution following removal of the CuBTTri-poly material.

4.2. Site Localized Delivery of Therapeutic NO Dosages

The in vivo effects of NO are concentration dependent resulting in protective and proliferative effects at low concentrations (0.1–10 nM), and cytotoxic effects at high concentrations (100 nM), requiring careful tuning of NO release properties to exhibit intended effects.[26] Since the rate of NO generation using CuBTTri is dependent upon the amount of available catalyst in the material, CuBTTri thereby provides a unique handle for mediating the surface flux of NO in CuBTTri-poly materials. The average surface fluxes from the 4% and 1% CuBTTri films are 1.87 ± 0.08 nM s^{-1} cm^{-1} and 0.77 ± 0.06 nM s^{-1} cm^{-1}, respectively, falling within the protective and proliferative therapeutic range.[27] Furthermore, we explored the effects of immersing CuBTTri-poly material in fresh citrated whole blood (37 °C, 30 min) on the reactivity of the material towards NO generation from CysamNO. Following immersion in blood, the CuBTTri-poly film was thoroughly rinsed with water and subsequently reacted with CysamNO in PBS to evaluate the materials capacity for generating NO. The resulting NO surface flux of the blood exposed CuBTTri-poly film (0.75 ± 0.08 nM s^{-1} cm^{-2}) remained consistent with the flux observed for the non-exposed film (0.77 ± 0.06 nM s^{-1} cm^{-2}), shown in Figure S3. These results provide the first demonstration that a MOF biocatalyst can retain its therapeutic action following exposure to biological fluids.

5. Conclusion

The development of biomedical devices which counter infection and the foreign body response through the generation of bioactive agents can extend the therapeutic lifetime of such important life-saving devices. In this work, we have described the use of a Cu-MOF as an implantable catalyst for the sustained generation of therapeutically essential levels of NO from bioavailable RSNO in physiological media. Contrary to previous inceptions of drug delivery vehicles, the use of an embedded catalyst liberates the materials dependence on the limited reservoirs of bioactive by relying on substrates (herein, RSNOs) supplied continuously in the physiological environment. The result is a resulting in a self-sustaining, therapeutic delivery system. In addition, tunable NO release kinetics were demonstrated based on the content of catalyst embedded into polymeric therapeutic materials. Most importantly, for the sustained use of the material, CuBTTri remains structurally intact in aqueous mediums including biological fluids, including whole blood, while retaining catalytic activity of the material. While rigorous in vitro and in vivo testing remains to be done to examine the full extent of the potential of CuBTTri in a therapeutic setting, this is the first report of a MOF which can catalytically generate a bioactive molecule from an endogenous source on the surface of a polymeric film with the capacity for tunable release kinetics in biological fluids.

6. Experimental Section

Materials: All reagents and solvents were purchased from commercial vendors and used without further purification unless otherwise noted. 1,3,5-tribromobenzene (98%), trimethylsilyl azide (94%), (trimethylsilyl)acetylene (98%), and diethylamine (99%) were purchased from Alfa Aesar. Cysteamine hydrochloride (Fluka, 99%), ethylenediaminetetraacetic acid (EDTA) disodium salt (EMD, 99%), copper iodide (Sigma, 99.5%), bis(triphenylphosphine) palladium(II) chloride (TCI America, 98%), copper chloride dihydrate (EMD, 99%), potassium carbonate (Fisher, 99%), and *t*-butyl nitrite (Sigma, 90%). Ultra high purity N_2 and O_2 gases were supplied by Airgas (Denver, Colorado) and solvents PBS tablets (Calbiochem) and Endothelial cell Media MCMD151 (Invitrogen) for the NOA measurements. Water was purified using a Millipore purification system set at 18 MΩ for all experiments.

CuBTTri Synthesis: *CuBTTri-*$H_2O{\cdot}H_3[(Cu_4Cl)_3(BTTri)_8(H2O)_{12}]{\cdot}72H_2O$.[1] 1,3,5-tris(1H-1,2,3-triazol-5-yl)benzene (225 mg) synthesized according to previously reported methods,[24] was dissolved in 30 mL DMF in a 120 mL vial. Triazole solution was adjusted to pH 4 with a dilute HCl solution. $CuCl_2{\cdot}2H_2O$ (383 mg) was dissolved in 10 mL DMF and added to triazole solution. Vial was placed in oven at 100 °C for 72 h followed by the reaction solution being kept at room temperature for 1 week. Resulting purple powder was centrifuged and washed with DMF 3 times. The percent yield of as synthesized CuBTTri-DMF was 75%. The powder was then placed in a Teflon lined Parr bomb along with 5 mL deionized water and heated in oven for 24 h at 100 °C. Purple powder was again centrifuged, washed with water and allowed to air-dry in hood for several days. Average particle size was determined to be 2.1 ± 0.5 μm.

Preparation of CuBTTri Films: Composite materials were prepared by dissolving 200 mg of Tygon polymer (S-50-HL) in 2 mL of THF. To the solvated polymer CuBTTri was added at 1 wt% (mg) and 4 wt% (mg). The CuBTTri polymer was cast into circular molds (radius of 2 mm) and allowed to cure under ambient conditions for 48 h. For NO release experiments the films were punched into 4 mm disks. Leaching analysis for each film was determined by the copper content found in the reaction solution following each experiment.

Preparation of CysamNO: A fresh stock solution of CysamNO was prepared in situ prior to each reaction. In brief, 0.05 M cysteamine hydrochloride was nitrosated with excess *t*-butyl nitrite. After reacting for 10 min under agitation in an ice bath, the concentration of the red CysamNO solution was determined by UV–Vis spectroscopy using characteristic absorption bands for RSNOs at 335 nm ($\varepsilon = 793\ M^{-1}\ cm^{-1}$) and 545 nm ($\varepsilon = 15\ M^{-1}\ cm^{-1}$).

Nitric Oxide Release Measurements: Nitric oxide generation was recorded in real time using a chemiluminescence based GE nitric oxide analyzer. To the NOA sampling vessel, 2 mL of PBS was added, where the PBS was treated with Chelex resin to remove trace amounts of Cu^{2+} ions and the pH was adjusted to 7.4. The catalyst CuBTTri (5×10^{-7} mol Cu^{2+}, 0.00018 g) or CuBTTRi films were added directly to the PBS solution and purged continuously for the duration of the experiment with ultrapure nitrogen gas. An aliquot of CysamNO was introduced directly into the solution in a gas tight Hamilton syringe through the side injection port of the NOA vessel. NO release was recorded in 1 s intervals as parts per billion with a gas sampling rate of 200 mL/min. Raw data was processed using Microsoft Excel 2010. The solution was maintained in a nitrogen atmosphere with bubbling of 16 mL/min N_2 directly into the solution and flow gas introduced at 184 mL/min into the remaining headspace, the system was continuously sampled under vacuum at 200 mL/min.

SEM Imaging and EDX Analysis of CuBTTri-Poly Films: Using a JEOL JSM-6500F (FSEM) with an accelerating voltage of 20.0 kV and a working distance of 10.1 mm. Images were taken at magnification values of 500× and 5000× and processed for copper distribution using EDX spectroscopy. The EDX spectrum was collected at an accelerating voltage of 20.0 kV at 130× magnification. All data was processed using Thermo NSS Release candidate 7 software.

Copper Leaching Studies: Inductively Coupled Plasma characterization was conducted on a Perkin Elmer Sciex DRC II. Table S1 (Supporting Information) displays pertinent information to ICP studies. A representative procedure is as follows: PBS (3 mL) was added to a 20 mL vial containing CuBTTri-H2O (5 mg). To this mixture 300 µL S-nitrosocysteamine was added. The vial was placed in a preheated sand bath at 37 °C for 12 hours. The mixture was then centrifuged and the supernatant was filtered through a syringe equipped with a 0.2 µm filter. Filtered solutions were then sent for Cu analysis.

Statistical Analysis: Statistical *t*-tests were performed on each data set to determine statistical differences at the 95% confidence interval.

Supporting Information

Supporting Information is available from the Wiley Online Library or from the author.

Acknowledgements

This research was supported by funds from the Boettcher Foundation's Webb-Waring Biomedical Research Program and Colorado State University.

Received: July 28, 2014
Revised: August 22, 2014
Published online: September 12, 2014

[1] a) P. Gilbert, A. J. McBain, A. H. Rickard, S. R. Schooling, in *Medical Biofilms*, John Wiley & Sons, Ltd, Chichester, UK **2003**, p 73; b) A. Vertes, V. Hitchins, K. S. Phillips, *Anal. Chem.* **2012**, *84*, 3858; c) J. W. Costerton, P. S. Stewart, E. P. Greenberg, *Science* **1999**, *284*, 1318.
[2] R. M. Donlan, in *Medical Biofilms*, John Wiley & Sons, Ltd, Chichester, UK **2003**, p 29.
[3] B. Jarvis, K. Simpson, *Drugs* **2000**, *60*, 347.
[4] a) T. A. Horbett, *Cardiovasc. Pathol.* **1993**, *2*, S137; b) M. A. Packham, *P. Soc. Exp. Bio. Med.* **1988**, *189*, 261.
[5] a) J. L. Harding, M. M. Reynolds, *Trends Biotechnol*. **2014**, *32*, 140; b) K. Bazaka, M. V. Jacob, R. J. Crawford, E. P. Ivanova, *Appl. Microbiol. Biot.* **2012**, *95*, 299.
[6] a) S. S. Gross, M. S. Wolin, *Annu. Rev. Physiol.* **1995**, *57*, 737; b) R. M. J. Palmer, A. G. Ferrige, S. Moncada, *Nature* **1987**, *327*, 524.
[7] a) C. Bogdan, *Nat. Immunol.* **2001**, *2*, 907; b) J. MacMicking, Q.-W. Xie, C. Nathan, *Annu. Rev. Immunol.* **1997**, *15*, 323.
[8] a) I. Sulemankhil, J. G. Ganopolsky, C. A. Dieni, A. F. Dan, M. L. Jones, S. Prakash, *Antimicrob. Agents Ch*. **2012**, *56*, 6095; b) A. B. Seabra, D. Martins, M. M. S. G. Simoes, R. da Silva, M. Brocchi, M. de Oliveira, *Artif. Organs* **2010**, *34*, E204.
[9] a) G. M. Annich, J. P. Meinhardt, K. A. Mowery, B. A. Ashton, S. I. Merz, R. B. Hirschl, M. E. Meyerhoff, R. H. Bartlett, *Crit. Care Med.* **2000**, *28*, 915; b) K. A. Mowery, M. H. Schoenfisch, J. E. Saavedra, L. K. Keefer, M. E. Meyerhoff, *Biomaterials* **2000**, *21*, 9.
[10] a) J. P. Cooke, *Artherosclerosis Supp.* **2003**, *4*, 53; b) M. K. Jones, K. Tsugawa, A. Tarnawski, D. Baatar, *Biochem. Bioph. Res. Co.* **2004**, *318*, 520.
[11] A. W. Carpenter, M. H. Schoenfisch, *Chem. Soc. Rev.* **2012**, *41*, 3742.
[12] R. M. J. Palmer, D. S. Ashton, S. Moncada, *Nature* **1988**, *333*, 664.
[13] a) Y. Zhang, N. Hogg, *Free Radical Bio. Med.* **2005**, *38*, 831; b) D. Giustarini, A. Milzani, R. Colombo, I. Dalle-Donne, R. Rossi, *Clin. Chim. Acta* **2003**, *330*, 85.
[14] a) R. J. Singh, N. hogg, J. Joseph, B. Kalyanaraman, *J. Bio. Chem.* **1996**, *271*, 18596; b) A. P. Dicks, D. L. H. Williams, *Chem. Bio.* **1996**, *3*, 655.
[15] a) S. C. Askew, D. J. Barnett, J. McAninly, D. L. H. Williams, *J. Chem. Soc. Perkin Trans. 2* **1995**, *8*, 741.
[16] a) S. Hwang, M. E. Meyerhoff, *Biomaterials* **2008**, *29*, 2443; b) B. K. Oh, M. E. Meyerhoff, *Biomaterials* **2004**, *25*, 283. c) S. C. Puiu, Z. Zhou, C. C. White, L. J. Neubauer, Z. Zhang, L. E. Lange, J. A. Mansfield, M. E. Meyerhoff, M. M. Reynolds, J. Biomed. *Mater. Res. Part B: Appl. Biomater.* **2009**, 203.
[17] a) J. R. Li, R. J. Kuppler, H. C. Zhou, *Chem. Soc. Rev.* **2009**, *38*, 1477; b) D. J. Collins, H. C. Zhou, *J. Mater. Chem.* **2007**, *17*, 3154.
[18] a) Y. Yu, Y. Ren, W. Shen, H. Deng, Z. Gao, *Trends in Anal. Chem.* **2013**, *50*, 33; b) J. R. Li, J. Sculley, H. C. Zhou, *Chem. Rev.* **2012**, *112*, 869.
[19] a) M. Yoon, R. Srirambalaji, K. Kim, *Chem. Rev.* **2011**, *112*, 1196; b) A. Corma, H. García, F. X. Llabrés i Xamena, *Chem. Rev.* **2010**, *110*, 4606.
[20] a) A. C. McKinlay, R. E. Morris, P. Horcajada, G. Ferey, R. Gref, P. Couvreur, C. Serre, *Angew. Chem. Int. Edit.* **2010**, *49*, 6260; b) P. Horcajada, R. Gref, T. Baati, P. K. Allan, G. Maurin, P. Couvreur, G. Ferey, R. E. Morris, C. Serre, *Chem. Rev.* **2012**, *112*, 1232; c) P. Horcajada, T. Chalati, C. Serre, B. Gillet, C. Sebrie, T. Baati, J. F. Eubank, D. Heurtaux, P. Clayette, C. Kreuz, J.-S. Chang, Y. K. Hwang, V. Marsaud, P.-N. Bories, L. Cynober, S. Gil, G. Ferey, P. Couvreur, R. Gref, *Nat. Mater.* **2010**, *9*, 172.
[21] a) O. M. Yaghi, M. O'Keeffe, N. W. Ockwig, H. K. Chae, M. Eddaoudi, J. Kim, *Nature* **2003**, *423*, 705; b) M. Eddaoudi, D. B. Moler, H. Li, B. Chen, T. M. Reineke, M. O'Keeffe, O. M. Yaghi, *Acc. Chem. Res.* **2001**, *34*, 319.

[22] a) G. Aromi, L. A. Barrios, O. Roubeau, P. Gamez, *Coordin. Chem. Rev.* **2011**, *255*, 485; b) J.-P. Zhang, Y.-B. Zhang, J.-B. Lin, X.-M. Chen, *Chem. Rev.* **2012**, *112*, 1001.
[23] J. L. Harding, M. M. Reynolds, *J. Am. Chem. Soc.* **2012**, *134*, 3330.
[24] A. Demessence, D. M. D'Alessandro, M. L. Foo, J. R. Long, *J. Am. Chem. Soc.* **2009**, *131*, 8784.
[25] T. M. McDonald, D. M. D'Alessandro, R. Krishna, J. R. Long, *Chem. Sci.* **2011**, *2*, 2022.
[26] a) A. C. McKinlay, B. Xiao, D. S. Wragg, P. S. Wheatley, I. L. Megson, R. E. Morris, *J. Am. Chem. Soc.* **2008**, *130*, 10440; b) P. N. Coneski, M. H. Schoenfisch, *Chem. Soc. Rev*. **2012**, *41*, 3753.
[27] H. Tapiero, D. M. Townsend, K. D. Tew, *Biomed. Pharmacother.* **2003**, *57*, 386.